Observation of sub-Poisson Franck–Hertz light at 253.7 nm

M. C. Teich and B. E. A. Saleh

Columbia Radiation Laboratory, Department of Electrical Engineering, Columbia University, New York, New York 10027

Received July 16, 1984; accepted October 5, 1984

We report the generation of ultraviolet (253.7-nm) sub-Poisson light from Hg vapor excited by inelastic collisions with a space-charge-limited (quiet) electron beam. This first stationary sub-Poisson light source is only weakly so, with a Fano factor that is between two and three standard deviations below that for Poisson light. This is principally because of optical losses in the experimental apparatus. There does not appear to be any fundamental limit that impedes the techniques from being used to produce an intense cw light source that is also arbitrarily sub-Poisson.

1. INTRODUCTION

Twenty years ago an important theoretical study on the quantum theory of light was carried out by Glauber.[1,2] One of the significant conclusions originating from this work is that quantum electrodynamics entertains a far broader variety of states of the electromagnetic field than does classical electrodynamics. Examples of light without classical analog include squeezed, antibunched, and sub-Poisson sources. Other manifestations of a nonclassical photon point process are also possible, e.g., an interevent-time probability density function whose coefficient of variation lies below unity. About 15 years ago, researchers began to ruminate about ways of generating quantum-mechanical light. Early suggestions originated with Mollow and Glauber[3,4] and with Stoler,[5,6] who studied squeezed states as well as the use of degenerate parametric amplification as a mechanism for producing antibunched light. Since that time, there have been many other suggestions for generating nonclassical light.[7] Almost all of these, in one way or another, involve higher-order (nonlinear) optical interactions, such as parametric amplification, multiphoton processes, and resonance fluorescence.

In a recent theoretical study we showed that, under proper circumstances, sub-Poisson light is expected to be generated by a system composed of sub-Poisson excitations cascaded with independent sub-Poisson nonstationary individual emissions.[8] As a specific method for constructing such a source, we proposed that a collection of atoms be excited by inelastic collisions with a low-energy space-charge-limited (quiet) electron beam.[9] In this scheme, the reduction of the usual Poisson randomness of the excitations arises from space-charge effects.[10–12] The quieting process in vacuum has been studied extensively, and it can be substantial.[12] Compact expressions exist for the shot-noise reduction factor Γ^2 (which carry over to the electron variance-to-mean ratio F_e); values of F_e smaller than 0.1 are typical, and values as low as 0.01 are possible. After excitation, each atom emits a (sub-Poisson) single photon by the Franck–Hertz (FH) effect.[13,14] The technique works by transferring the anticlustering properties of the electrons, resulting from Coulomb repulsion, to the photons. The direction of transfer is the inverse of that encountered in the usual photodetection process, in which the statistical character of the photons is imparted to the photoelectrons.

A. Photoemission and Inverse Photoemission

A comparison between photoemission and inverse photoemission is schematically illustrated in Fig. 1. For photoemission, in Fig. 1(a), a photon impinges upon a metal or atom and liberates an electron. The maximum kinetic energy of the electron (KE_{max}) is equal to the photon energy ($h\nu$) minus the work function of the material ($e\phi$) in accordance with Einstein's photoelectric equation, as shown in Fig. 1(b). The flux relation displayed in Fig. 1(c) demonstrates that the average photocurrent i_e is proportional to the average photon flux (I). Finally, sample functions of the photon point process (excitation statistics) and the resulting electron point process (final statistics) are represented in Fig. 1(d). They are related by a Bernoulli transform that results from the nonunity quantum efficiency of the photodetector (this is random deletion, which is also known as partition noise).

The processes are essentially reversed for inverse photoemission (the Franck–Hertz effect). In Fig. 1(a), an electron strikes an atom, loses its kinetic energy, and excites the atom. The atom then decays to a lower energy state and in the process emits a single photon by spontaneous emission. The energy of the emitted photon is equal to the energy supplied to the electron by an external field (E) less the cathode-emitter contact potential $e\theta$, as shown in Fig. 1(b). Only electrons with kinetic energy corresponding to the discrete energy levels of the atom (indicated by crosses) are effective in producing photons. In Fig. 1(c) we show that the average photon flux is proportional to the average electron current. Because this mechanism involves ordinary spontaneous emission, it is a first-order optical process and can be expected to produce a high photon flux. Finally, in Fig. 1(d) we illustrate the electron point process (excitation statistics). It is portrayed as quite regular because of the space-charge regularization. The photon point process (final statistics) is a Bernoulli-deleted version of the electron point process as a result of optical loss. This is the essential limiting factor in generating sub-Poisson light by this (or any other) scheme. Partition noise and/or additive independent Poisson events dilute sub-Poisson behavior and relentlessly move the

0740-3224/85/020275-08$02.00

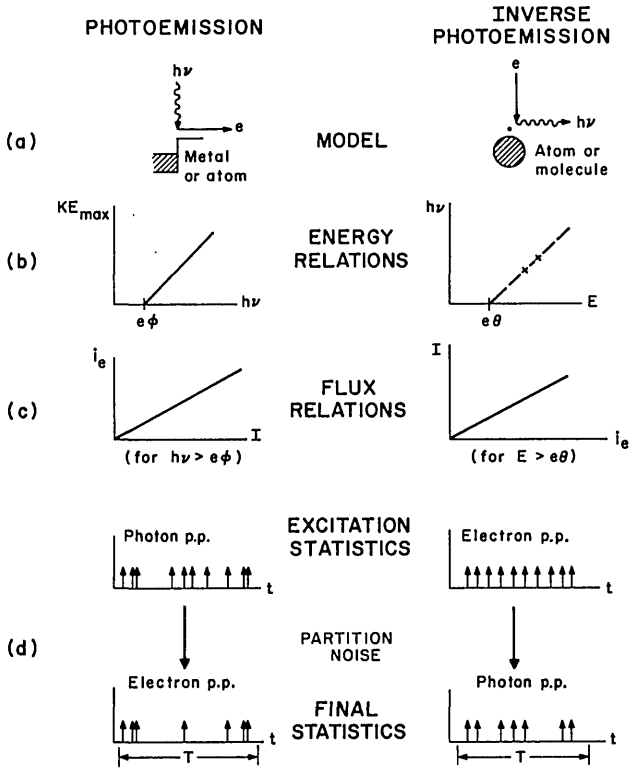

Fig. 1. Schematic representation of photoemission and inverse photoemission (Franck–Hertz effect). Electrons and photons behave like classical particles in photon counting, provided that $M_s \gg 1$, $T \gg \tau_p, \tau_e$.

counting statistics toward the Poisson.[15–17] Nevertheless, the sub- or super-Poisson state of a source of light is conserved under the effects of such partition noise.[16,17]

B. Earlier Experimental Work

There have been few cases in which nonclassical light has been generated in the laboratory. A number of relevant two-beam experiments have been discussed by Loudon.[7] More recently, Kimble *et al.*[18–20] used laser-excited resonance fluorescence radiation from Na vapor as a means of producing antibunched light. Similar results were achieved by Walther and his coworkers.[21] In 1983, again using resonance fluorescence, Short and Mandel[22] observed sub-Poisson individual emissions from isolated Na atoms. They selectively counted the fluroescence photons when only one atom was in the field of view of their apparatus and determined that the results were sub-Poisson. Constructing a sub-Poisson light source from a *collection* of such emissions is difficult, however, because the excitation statistics (the arrival of the atoms) must also be made sub-Poisson.[8] In the experiment conducted by Short and Mandel, these statistics are determined by the number of atoms in the field of view, and there is no simple way in which this number can be regulated.[23] If the atoms arrive in Poisson fashion, as expected, the resulting stationary source of light produced will in fact be super-Poisson.[8,15] One way in which it may be possible to reduce atomic fluctuations is by using two-level ions (rather than neutral atoms). The mutual ionic Coulomb repulsion could then serve to provide a sub-Poisson number of atoms in the field of view.

It is important to point out that can be observed in a short-time sub-Poisson photon statistics window by simply choosing when to look. An example is provided by a modified version of the experiment recently performed by Aspect *et al.*[24] Two photons emitted from a single atom (the $4p^2\,{}^1S_0 \rightarrow 4s4p\,{}^1P_1 \rightarrow 4s^2\,{}^1S_0$ cascade in ^{40}Ca) were used in an elegant polarization correlation experiment to demonstrate a strong violation of the generalized Bell inequalities.[25] Instead of a coincidence experiment, we consider a photon-counting experiment in which the registration of the upper (green) photon triggers a photon counter maximally sensitive to the lower (violet) photon. It is clear that the violet photon will arrive in Bernoulli fashion, representing a sub-Poisson nonstationary individual emission. Individual spontaneous atomic emissions are single photons that may or may not be detected. As such, they are clearly sub-Poisson in an appropriate time window. Resonance fluorescence photon clusters are likely to be less sub-Poisson than single-photon emissions because of the added randomness associated with the number of photons in the cluster. The trick is to produce a *stationary* source of sub-Poisson light.[26]

In this paper, we report the observation of ultraviolet (253.7-nm) sub-Poisson light from Hg vapor excited by inelastic collisions with a space-charge-limited electron beam. This first stationary sub-Poisson light source is only weakly so (with a Fano factor that is between two and three standard deviations below that for Poisson light) principally because of optical losses in the experimental apparatus. From a theoretical point of view, there are no obvious fundamental barriers to producing an arbitrarily quiet intense cw source by using this method. Quiet light may find use in applications such as optical signal processing and optical communications. It could be useful for investigating optical interactions in various disciplines, such as the behavior of the human visual system at the threshold of seeing.[27] It should be noted that a sub-Poisson source may or may not be antibunched.[9] A preliminary report of this work was presented at the Thirteenth International Quantum Electronics Conference in Anaheim, California.[28]

2. EXPERIMENT

A. Apparatus

A block diagram of the experimental apparatus is shown in Fig. 2. A specially constructed FH tube is placed in a rectangular metal enclosure that serves as both an oven and a shield, thereby minimizing electrical and electromagnetic interference. An ultraviolet-transmitting, visible-attenuating filter (Schott UG-5) permits the FH light to pass out of the enclosure while attenuating some of the red and infrared filament light from the FH tube. The radiation impinges upon a photon-counting photomultiplier tube (PMT) about 3 cm away from the center of the FH tube. The PMT (Hamamatsu R431SP) was specially selected for high quantum efficiency at 253.7 nm (≈15%) and was operated at ambient temperature. It is inserted in a special base (Hamamatsu C1050) that provides preamplification, discrimination, and pulse shaping and supplies high voltage to the PMT (1025 V from an Ortec 456). The output is then passed through a buffer amplifier (5×) to convert the C1050 output to standard TTL pulses. The standardized signal goes to the electronic photon-counting equipment. Both a rate photon counter (Hewlett-Packard 5370A) and a statistical photon counter

(Langley-Ford 1096) are used; the latter is controlled by a Hewlett-Packard minicomputer (HP 9825B). The rate photon counter provides the detected mean photon count rate μ in thousands of counts per second (kcnt/sec), whereas the statistical photon counter gives the probability distribution $p(n, T)$ for the detection of n photons in the time T. The mean photon count $\langle n \rangle$ and the count variance-to-mean ratio (Fano factor) $F_n(T)$ are calculated from $p(n, T)$. The entire apparatus, except for the photon counters and computer control, is placed on a metal vibration-isolation table. The FH source, the laser, and the PMT are in a light-tight box.

The FH tube was specially constructed in a Corning 9741 cylindrical envelope (52-mm height, 25-mm diameter, 0.8-mm wall thickness) to permit the ultraviolet light to emerge. The filament/BaO-cathode assembly is encased in a cylindrical Ni enclosure with a 5-mm orifice at the top that serves as the first grid (G1). This assembly is a modified version of a standard vidicon unit. The filament voltage was supplied by a 12-V dc Pb storage battery to minimize noise. A decade resistance box was placed in series with the battery to provide a filament voltage of 6.05 V dc. For the experiments reported here, the cathode was electrically connected to the negative-polarity side of the filament; both G1 and the envelope of the tube were set at ground potential. Two circular Ni meshes (90% light transmission) serve as the second grid (G2) and anode (A), located 10 and 14 mm away from G1, respectively. For this set of experiments the tube was used as a diode, i.e., the two meshes were connected together to serve as a single anode, as indicated schematically in Fig. 2. The tube is filled with 0.75-g pure natural Hg. A semicylindrical Al mirror is coated on the exterior of the upper portion of the tube to enhance light collection. Al foil is wrapped about the top of the tube for this same purpose. Electrical measurements confirmed the presence of the classic FH dip in the anode current (when operated in the proper configuration and at sufficiently high temperature) and the presence of space charge in the tube.[11] Simultaneous electrical and optical experiments were avoided because of bursts of noise introduced by the current-measuring electrometer (Keithley 610C) at the low levels of operation (picoamperes).

The oven was heated to the desired temperature by applying 50-V dc to the oven coil through a temperature controller (Love 49J). Feedback to the controller is provided by a lug thermocouple mounted in the oven. The temperature is maintained constant to better than 0.1°C and is recorded by a digital thermometer (Keithley 871). Most experiments were conducted either at ambient temperature (26.6°C) or in the range 90–120°C; the sub-Poisson behavior seems to be most pronounced at these temperatures.

B. Parameters

Experimental parameters and values were determined in the following way. The 6.05-V filament voltage and the diode configuration of the tube provided substantial space charge as determined from electrical measurements. The electron Fano factor is estimated to be $F_e \approx 0.1$ based on typical vacuum-tube results.[12] The tube was operated at 26.6°C, where the system exhibited its lowest noise operation and highest PMT efficiency. This low temperature also minimized the effects of resonance trapping and Hg excimer production. The electron–atom excitation probability η_e is estimated to be ≈ 0.25 at this temperature; electrical measurements showed that this factor approaches 0.9 at roughly 90°C. The tube was placed as close as practicable (≈ 3 cm) to the PMT, and with the surrounding Al foil and semicylindrical mirror, we estimate that the geometrical photon-collection efficiency $\eta_g \approx 0.1$. Many spatial modes were collected ($M_s \gg 1$) to eliminate wavelike noise[15] resulting from interference.[8] The transmission factor for the Schott UG-5 filter was measured to be $\eta_f = 0.83$ at 253.7 nm. The UG-5 transmission for 6.05-V filament light was 0.28; these numbers play a role in determining the level of additive Poisson light. The discriminator setting on the PMT base was adjusted to 1.0 V to balance between the effects of excessive PMT afterpulsing and cosmic-ray events on the one hand and the loss of counting efficiency on the other hand. The counting time T was set at 1.0 μsec. This was short enough to provide a large number of samples (and therefore good statistics) and to minimize afterpulse and cosmic-ray-induced photoelectron clusters,

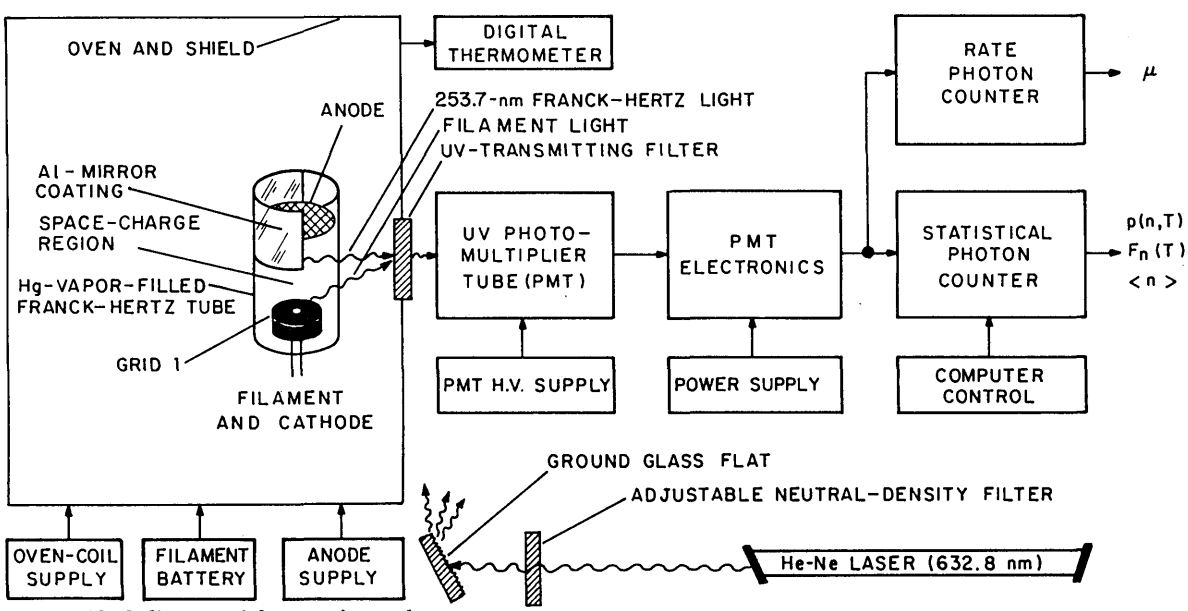

Fig. 2. Block diagram of the experimental arrangement.

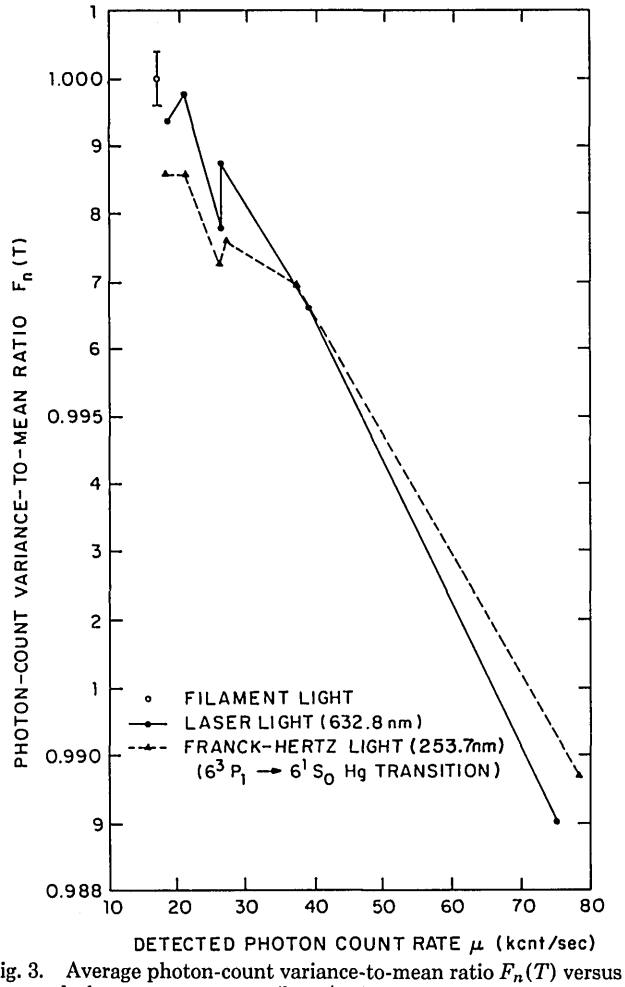

Fig. 3. Average photon-count variance-to-mean ratio $F_n(T)$ versus detected photon count rate μ (kcnt/sec) for experiment 0323:3-15. Raw data are shown for Poisson filament light (open circle), Poisson laser-plus-filament light (solid circles and solid line segments), and sub-Poisson FH-plus-filament light (triangles and dashed line segments). Each data point is based on approximately 10^7 samples. The error bracket is the same for all data points. The Fano factors for FH light are seen to lie below those for Poisson light at sufficiently small values of the count rate. The overall negative slope of the data is due to dead time in the photon-counting apparatus. Numerical parameter values are given in Table 1.

which raise the Fano factor above unity. On the other hand, T must be set as high as possible in order to capture the anticorrelated events, i.e., to satisfy the conditions $T \gg \tau_p, \tau_e$, where τ_p is the photon excitation/emission correlation time and τ_e is the electron correlation time.[8] The mean count $\langle n \rangle$ was kept low to avoid both saturation of the PMT (and its associated electronics) and large dead-time effects[29,30] in the counting system. $\langle n \rangle$ was maintained sufficiently high, however, to overbalance the Poisson filament light and to maintain $T \gg \tau_e$. The PMT quantum efficiency $\eta_p \approx 0.15$, as mentioned previously. An estimate for the losses owing to subsidiary effects such as photoemission, resonance trapping, photoluminescence, and excimer production (see Section 3) is ≈20%, so that the associated quantum efficiency $\eta_s \approx 0.8$. The overall quantum efficiency η (the product of the aforementioned individual quantum efficiencies) therefore turns out to be ≈0.0025. This is the principal culprit that results in an effect of small magnitude.

C. Paradigm

The object of the experiments was to observe sub-Poisson behavior, i.e., a count variance-to-mean ratio less than unity. Sets of photon-counting measurements were carried out for the FH light, as well as for pure filament light from the FH tube, and for 632.8-nm He–Ne laser light (Coherent 80-2SPA), which served as a comparison source. Filament light was present together with both the FH light and the laser light. First, a set of measurements was performed for the filament light alone. A set consisted of 50 photon-counting distributions, each with counting time $T = 1.0$ μsec and duration 0.4 sec. Because of the duty cycle of the photon counter (≈0.5), each distribution contained $\approx 2 \times 10^5$ events. An entire set, which took about 100 sec to collect because of data readout time between distributions, typically consisted of $N \approx$ 10,061,600 samples. Relative frequency distributions for the mean count and the Fano factor across the 50 distributions were constructed. The mean Fano factor $F_n(T)$ is the datum of interest (see open circle in Fig. 3). The data were collected in 0.4-sec slices to minimize the effects of slow sensitivity and gain variations in the system. In some experiments the data collection was not divided in this fashion, and a single counting distribution was collected for a period of 20–30 sec ($N \approx 10$–15×10^6). The results were similar. The standard error (SE) for a measurement of $F_n(T)$ that consists of 10^7 samples turns out to be $\approx (2/N)^{1/2} \approx 0.0004$. This calculated value for the SE was verified experimentally by carrying out many series of runs. It is indicated by the error bracket in Fig. 3, which applies to all data points.

After the datum for the filament light was obtained, the anode voltage on the FH tube was increased until the desired photon count rate $\mu = \langle n \rangle / T$ was observed on the rate photon counter. The onset of ultraviolet light emission occurs when the anode supply voltage v_A exceeds about 5.9 V dc (the photon energy plus the contact potential). μ increases steeply with v_A ($\mu \approx 10^5$ when $v_A \approx 6.7$ V dc), so that typical values of v_A used in our experiments were in the range 6.0–6.5 V dc. The use of a regulated dc power supply (Lambda LL-905), rather than a battery, for the anode supply reduced drift in the anode current. For a given value of $\langle n \rangle = \mu T$, a set of 50 photon-counting distributions was collected in the manner described above, and the mean Fano factor for the FH light was plotted as a triangular data point in Fig. 3. The value of μ was then changed, for example by decreasing v_A slightly, until the new desired value of μ was achieved, at which point the statistical photon counter was used to collect 50 photon-counting distributions (another data point) for the FH-plus-filament light. Values for the observed mean Fano factors $F_n(T)$ (triangles) are connected by the dashed line segments in Fig. 3. The large admixture of Poisson filament light present in the FH light at low levels of μ decreases with increasing μ.

Actually, the measurement of each of these FH-plus-filament data points was alternated with a measurement using filament light together with He–Ne laser light scattered from a ground-glass flat (filled circles connected by solid line segments in Fig. 3). This mitigated the effects of slow system gain variations that were occasionally observed. An adjustable neutral-density filter provided a value of μ comparable with that of the previous FH measurement. Because of afterpulsing and dead-time effects, it is *essential* to compare the FH light experimentally with a Poisson photon source

(rather than with a theoretical Poisson distribution) at each μ. The filament-plus-laser light can be shown to provide an excellent Poisson photoelectron distribution because of the short counting time and the extremely low value of the PMT quantum efficiency for light at these wavelengths. Calculations show that the first factor reduces any wavelike fluctuations present in the filament-plus-laser light to unmeasurable proportions, whereas the second factor similarly reduces any particlelike fluctuations.[16] To confirm experimentally the Poisson nature of the laser light, we determined that the linear regression line for the Fano factors obtained from the filament light was identical with that obtained from the filament-plus-laser light.

3. RESULTS

A. Raw Data

A representative set of raw data for the average photon-count variance-to-mean ratio $F_n(T)$ versus the detected photon count rate μ (kcnt/sec) is shown in Fig. 3 for experiment 0323:3-15. Data are shown for Poisson filament light (open circle), Poisson filament-plus-laser light (solid circles and solid line segments), and sub-Poisson FH-plus-filament light (triangles and dashed line segments). The error bracket (± 0.0004) is the same for all data points. In the range $\mu < 30$ kcnt/sec ($\langle n \rangle < 0.03$), values of the Fano factor for the F–H light lie below those for the Poisson light by between two and three standard deviations (depending on the details of how the estimates are made; see Table 1 for values of some specific data points). Low μ corresponds to low degeneracy parameter (note that the parameter μ used here is to be distinguished from the parameter μ used in Ref. 8). Only relative measures of $F_n(T)$ carry meaning; absolute measurements mean little because of afterpulsing and dead time in the counting system, as is discussed in Subsection 3.B.

At higher count rates, the data in Fig. 3 indicate that the FH light appears to be noisier than the Poisson light. We have carried out many such experiments and consistently see this behavior. There are several reasons why this may occur; these include the diminished role that dead time plays for sub-Poisson processes (this would make it *appear* that the FH light is noisier), the increase in the degeneracy parameter of the light,[8] and the possibility of stimulated photoluminescence. We have determined experimentally that exposure of the FH tube envelope to a strong source of radiation at 253.7 nm does indeed lead to substantial phosphorescence.

In Fig. 4 we present the normalized photon-counting distribution $[n!p(n)$ versus count number $n]$ obtained from a collection of 50 photon-counting measurements from experiment 0504:2-3. The dashed line segments represent results for FH-plus-filament light, whereas the solid line segments represent the distribution for Poisson light. The sub-Poisson nature of the FH light can just barely be discerned for $2 \leq n \leq 4$ (the binomial law was used to calculate the error brackets). Greater accuracy is available from the Fano factor provided in Fig. 3 because it combines the deviations from Poisson behavior for all n values into a single parameter. Numerical values associated with Fig. 4 are provided in Table 1. They are seen to be similar to comparable data from experiment 0323:8-7, also presented in Table 1.

B. Corrections to the Data

There are a number of corrections that must be applied to the raw data if we wish to obtain an absolute value of $F_n(T)$ for the FH light. These include afterpulsing and cosmic-ray events in the PMT, dead time in the photon-counting system, and background counts from the filament. Because of the well-known properties of modified Poisson processes, the magnitudes of these effects can be estimated quite readily from the Poisson-light data points. However, it is difficult to apply these corrections in a proper way to the FH light because the characteristics of the underlying point process are not known. The problem is particularly difficult because of the admixture of Poisson filament light in the FH light. Rather than attempting to make such corrections analytically, therefore, we have measured the value of $F_n(T)$ for the FH light relative to that for Poisson light. To be able to treat the data in this manner requires the plausible assumption that afterpulsing and dead time distort the FH and Poisson light in approximately the same way. Indeed, if anything, dead time will affect the Poisson light more than the FH light, thereby making the sub-Poisson nature of the FH light appear to be less significant than it actually is. The experimental procedure that we used is essentially equivalent to normalizing these effects out of the system.

Table 1. Comparison of Uncorrected and Corrected Fano Factors for Experiments with Comparable Count Rates

Source	Photon Count Rate μ[a]	Fano Factor $F_n(T)$ at $\mu \approx 26\,000$[b]	ΔF_n at $\mu \approx$ 26 000	Regression-Line Intercept $F_n(\mu \to 0)$[c]	Corrected Fano Factor $F_n'(\mu \to 0)$[c,d]	$\Delta F_n'$ $(\mu \to 0)$[e]	$\Delta F_n'$ (Theory)
Poisson light (experiment 0323:8)	26119	0.99876		1.0032	1.0000		
			−0.00112			−0.0016	−0.0007
FH + filament light (experiment 0323:7)	26871	0.99764		1.0016	0.9984		
Poisson light (experiment 0504:2)	26268	0.99829					
			−0.00084				−0.0007
FH + filament light (experiment 0504:3)	26256	0.99745					

[a] Data with approximately the same count rate were chosen for comparison.
[b] Fano factors in this table all have a standard error $\approx (2/N)^{1/2} \approx \pm 0.0004$.
[c] The effects of dead time are corrected by determining the regression-line intercept at $\mu = 0$.
[d] Spurious afterpulses and cosmic-ray events are corrected by using the afterpulse probability determined from the Poisson data ($q \approx 1.6 \times 10^{-3}$ for any given pulse in $T = 1$ μsec).
[e] Background light is not removed, so the sub-Poisson effect is underestimated.

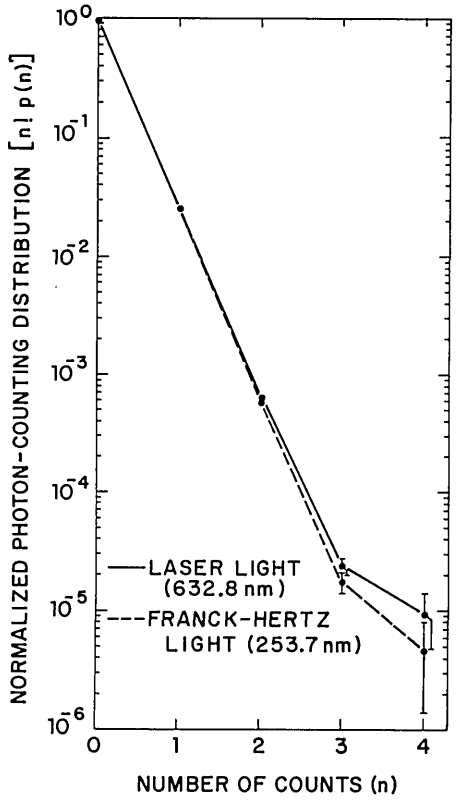

Fig. 4. Normalized photon-counting distribution $[n!p(n)]$ versus count number n for experiment 0504:2-3. Raw data are shown for Poisson laser-plus-filament light (solid line segments) and sub-Poisson FH-plus-filament light (dashed line segments). Numerical values for the photon count rates and Fano factors are presented in Table 1.

In spite of the fact that we may not use them with utter confidence, there is benefit in calculating the magnitudes of the aforementioned corrections, and we proceed to do so. To obtain values for the probability of an afterpulse in the PMT, and the magnitude of the dead time in the counting system, a linear regression line was constructed for the Poisson light data. (This procedure also allowed us to confirm experimentally the statistical reliability of the Fano factor, as mentioned earlier.) The results were substantially the same whether or not the highest-rate data point shown in Fig. 3 was included in the regression calculation; we report the calculation in which all seven circular data points were used. Essentially, the zero-rate intercept of the regression line reflects excess event clustering resulting principally from afterpulsing in the PMT, whereas its negative slope reflects system dead time. For Poisson light the intercept was $F_n(\mu \to 0, \text{Poisson}) = 1.0032$. If we assume that for every PMT pulse there is a Bernoulli-distributed probability of an additional spurious pulse, the afterpulse probability q is calculated to be

$$q = (F_n - 1)/(3 - F_n). \tag{1}$$

From Eq. (1), the numerical value of q is $\approx 1.6 \times 10^{-3}$ for any given pulse in $T = 1$ μsec.

The magnitude of the dead time is determined by the slope of the regression line, which turns out to be $m(\text{Poisson}) = -1.8567 \times 10^{-7}$. We make use of the well-known relations for the nonparalyzable dead-time-modified Poisson (DTMP) distribution (the Langley-Ford statistical photon counter operates by a mechanism similar but not identical to this mathematical process). The relationship between the Fano factor for this distribution, F_{DTMP}, the observed count rate μ, and the nonparalyzable dead time τ_d is[8,29,30]

$$F_{\text{DTMP}} \approx (1 - \mu\tau_d)^2. \tag{2}$$

Equation (2) should not be used directly to determine τ_d because of the excess clustering in the unmodified process. Rather, the dead time may be estimated accurately from the derivative of this equation:

$$dF_{\text{DTMP}}/d\mu \approx -2\tau_d + 2\tau_d{}^2\mu \approx -2\tau_d, \tag{3}$$

which leads to an expression for the dead time given by

$$\tau_d \approx -\tfrac{1}{2}m(\text{Poisson}). \tag{4}$$

Inserting the measured value for $m(\text{Poisson})$, we estimate that $\tau_d \approx 92.8$ nsec, in rough accord with the instrumental resolution specified by the manufacturer.

We now report values for the regression-line intercept and slope for the FH-plus-filament light and attempt to reduce the data in a rather crude way. These were found to be $F_n(\mu \to 0, \text{sub-Poisson}) = 1.0016$ and $m(\text{sub-Poisson}) = -1.4921 \times 10^{-7}$, respectively. If we do not correct for the background filament light, we can use the above-derived value of q together with the Burgess variance theorem[16] to calculate a corrected Fano factor $F_n'(\mu \to 0, \text{sub-Poisson})$ for the FH-plus-filament light in the absence of afterpulsing and dead time. Calculations yield $F_n'(\mu \to 0, \text{sub-Poisson}) \approx 0.9984$. Correcting for the substantial background flux ($\mu_{\text{Fil}} = 16.582$ kcnt/sec) would, of course, provide a lower estimate for the true value of $F_n'(\mu \to 0, \text{sub-Poisson})$.

In Table 1 we compare the uncorrected and corrected Fano factors for two sets of data (experiments 0323:7–8 and 0504:2–3) that have nearly the same count rate ($\mu \approx 26000$). The quantities ΔF_n and $\Delta F_n'(\mu \to 0)$ represent differences between the FH-plus-filament light Fano factor and the Poisson-light Fano factor. We have already pointed out that the uncorrected FH Fano factors lie below those for Poisson light by between two and three standard deviations (since the error bracket is the same for all data points, ±0.0004). It is clear from Table 1 that the margin may increase to four standard deviations when corrections for afterpulsing and dead time are included. If it were known how to correct for the background filament light, the margin would be yet greater.

C. Comparison with Theory

We have calculated the theoretical Fano factor and counting distribution for space-charge-limited electron-excited FH light under various conditions.[8,9,16,17] In the long-counting-time limit and in the absence of interference (e.g., when the emissions are instantaneous and/or when many spatial modes are detected), the photons behave as classical particles, and the expected Fano factor is

$$F_n = 1 - \eta\beta(1 - F_e), \qquad T \gg \tau_p, \tau_e; M_s \gg 1. \tag{5}$$

Here η is the overall quantum efficiency from electrons to detected photons ($\eta = \eta_e\eta_g\eta_f\eta_p\eta_s$). The quantity β accounts for the admixture of independent Poisson light [$\beta = (1 + \langle r\rangle/\langle s\rangle)^{-1}$, where $\langle r\rangle$ and $\langle s\rangle$ are the detected Poisson and pure FH count means, respectively].[16,17] F_e, of course, is the Fano factor for the exciting electrons. Numerical estimates for these quantities provide $\eta \approx 0.0025$, $\beta \approx 0.3$, and $F_e \approx 0.1$. The theory cited above incorporates neither afterpulsing nor

dead time, so that the theoretical value of $-\eta\beta(1-F_e)$ is the expected deviation of the Fano factor for FH light relative to a measurement of the Fano factor for Poisson light. The numerical estimate for $\Delta F_n'$(theory) turns out to be ≈ -0.0007, which is roughly two standard deviations below the mean and is close to the observed value (see Table 1).

We note that full counting distributions such as that displayed in Fig. 4 were usually recorded, but we use the Fano factor as a simple and more accurate measure of the sub-Poisson character of the light. It is useful because it succinctly describes the noisiness of the source relative to that of an ideal amplitude-stabilized laser.

Finally, we briefly discuss a number of subsidiary effects that occur in the course of FH light generation. The 253.7-nm photons interact with the Hg atoms themselves and with the metal and glass parts of the tube. This results in resonance trapping,[31] photoelectric effect, and photoluminescence, respectively. Resonance trapping extends the lifetime of the state, causing some of the anticorrelated photons to fall in a delayed time window, and thereby reduces the magnitude of the sub-Poisson effect. It also causes increased loss because of the extended pathlength traveled by each photon. Photoemission and photoluminescence also result in losses, the former by conversion of photons to electrons and the latter by delay to a later time window. Last, the production of excimers (dimers and trimers) results in visible light emission[32,33] and the consequent delay and loss of photons in the sensitive range of the PMT.

4. CONCLUSION

We conclude that the FH effect stimulated by a space-charge-limited electron beam is a source of sub-Poisson light, within the statistical uncertainties of the experiment. The agreement with theory is reasonable. We emphasize that there appear to be no fundamental obstacles preventing such a source from being arbitrarily strong and sub-Poisson. Indeed, the intensity of our source was carefully controlled so that the photon-counting equipment would measure the nonclassical nature of the light with a minimum of saturation and dead-time effects. A small increase in the anode voltage produces a virtual flood of photons. The effect that we observe is a stationary one. As such, it must be clearly distinguished from sub-Poisson behavior in individual atomic emissions, which depend on a careful choice of the time window and are obviously severely limited in strength.

There are a number of interesting related experiments, e.g., the use of a broad variety of higher atomic excited states, as well as other atomic, ionic, and molecular species, in a similar configuration. Thus there is the possibility of producing radiation with antibunched and sub-Poisson photon statistics in various regions of the electromagnetic spectrum, including the x-ray. Other charged particles could also be used as the excitation. Excited ionic species, subject to Coulomb repulsion because of their charge, could be used to generate sub-Poisson spontaneous emissions. A solid-state implementation of this effect may also be possible, since space-charge-limited electron currents and photon emission are both well-known processes in semiconductor devices.

Since most proposals to produce nonclassical light involve higher-order optical processes, it may be worthwhile to mention two possible multiple-photon versions of the current experiment. The first is a multiphoton FH effect in which the electron excites an atomic state that can decay only by means of spontaneous two-quantum emission. This process is the inverse of the multiphoton photoelectric effect.[34] If such an effect could be observed, the photon flux would be extremely low, and, in any case, the nonclassical nature of the source would be diluted by the multiplication process. The second possibility is more interesting. It involves a sub-Poisson electron-excited FH experiment in which the accelerating voltage is increased to the point at which two (or more) light bands are produced; i.e., to a value at which each electron produces two spatially separated and time-separated photons. This technique yields twice the light for the same number of electrons,[33] but again, the multiplication dilutes the sub-Poisson property. However, the two bands might serve as an interesting nonclassical Young double-slit source because of photon anticorrelations at the two slits.[8]

ACKNOWLEDGMENTS

This research was supported by the Joint Services Electronics Program (U.S. Army, U.S. Navy, and U.S. Air Force) under contract DAAG29-82-K-0080 and by the National Science Foundation under grant ECS-82-19636. We are indebted to Todd Larchuk for superb technical assistance.

B. E. A. Saleh is also with the Department of Electrical and Computer Engineering, University of Wisconsin, Madison, Wisconsin 53706.

REFERENCES

1. R. J. Glauber, "The quantum theory of optical coherence," Phys. Rev. **130,** 2529–2539 (1963).
2. R. J. Glauber, "Coherent and incoherent states of the radiation field," Phys. Rev. **131,** 2766–2788 (1963).
3. B. R. Mollow and R. J. Glauber, "Quantum theory of parametric amplification. I," Phys. Rev. **160,** 1076–1096 (1967).
4. B. R. Mollow and R. J. Glauber, "Quantum theory of parametric amplification. II," Phys. Rev. **160,** 1097–1108 (1967).
5. D. Stoler, "Equivalence classes of minimum uncertainty packets," Phys. Rev. D **1,** 3217–3219 (1970).
6. D. Stoler, "Photon antibunching and possible ways to observe it," Phys. Rev. Lett. **33,** 1397–1400 (1974).
7. A number of review papers on this topic have appeared recently. For example, see R. Loudon, "Non-classical effects in the statistical properties of light," Rep. Prog. Phys. **43,** 913–949 (1980); H. Paul, "Photon antibunching," Rev. Mod. Phys. **54,** 1061–1102 (1982). See also J. Peřina, *Coherence of Light*, 2nd ed. (Reidel, Dordrecht, The Netherlands, 1984); *Quantum Statistics of Linear and Nonlinear Optical Phenomena* (Reidel, Dordrecht, The Netherlands, 1984).
8. M. C. Teich, B. E. A. Saleh, and J. Peřina, "Role of primary excitation statistics in the generation of antibunched and sub-Poisson light," J. Opt. Soc. Am. B **1,** 366–389 (1984).
9. M. C. Teich, B. E. A. Saleh, and D. Stoler, "Antibunching in the Franck–Hertz experiment," Opt. Commun. **46,** 244–248 (1983).
10. O. W. Richardson and C. B. Bazzoni, "Experiments with electron currents in different gases. (1) Mercury vapour," Phil. Mag. Ser. 6, **32,** 426–440 (1916).
11. J. Franck and P. Jordan, "Anregung von Quantenspruengen durch Stoesse," in *Struktur der Materie in Einzeldarstellungen, III* (Springer-Verlag, Berlin, 1926).
12. B. J. Thompson, D. O. North, and W. A. Harris, "Fluctuations in space-charge-limited currents at moderately high frequencies," RCA Rev. **4,** 269–285, 441–472 (1940); **5,** 106–124, 244–260 (1940); **5,** 371–388, 505–524 (1941); **6,** 114–124 (1941).
13. J. Franck and G. Hertz, "Ueber Zusammenstoesse zwischen Elektronen und den Molekuelen des Quecksilberdampfes und die Ionisierungsspannung desselben," Ver. Dtsch. Phys. Ges. **16,** 457–467 (1914).

14. J. Franck and G. Hertz, "Ueber die Erregung der Quecksilber-resonanzlinie 253,6 $\mu\mu$ durch Elektronenstoesse," Ver. Dtsch. Phys. Ges. **16**, 512–517 (1914).
15. B. E. A. Saleh, D. Stoler, and M. C. Teich, "Coherence and photon statistics for optical fields generated by Poisson random emissions," Phys. Rev. A **27**, 360–374 (1983).
16. M. C. Teich and B. E. A. Saleh, "Effects of random deletion and additive noise on bunched and antibunched photon-counting statistics," Opt. Lett. **7**, 365–367 (1982). In this reference, the definition of antibunching was taken to be identical with that of sub-Poisson. The definition of antibunching used in the current work [$g^{(2)}(0) < 1$] is in accord with the more usual usage of the term. The relationship between antibunching and sub-Poisson behavior is elucidated in Ref. 9.
17. J. Peřina, B. E. A. Saleh, and M. C. Teich, "Independent photon deletions from quantized boson fields: the quantum analog of the Burgess variance theorem," Opt. Commun. **48**, 212–214 (1983).
18. H. J. Kimble, M. Dagenais, and L. Mandel, "Photon antibunching in resonance fluorescence," Phys. Rev. Lett. **39**, 691–695 (1977).
19. H. J. Kimble, M. Dagenais, and L. Mandel, "Multiatom and transit-time effects on photon-correlation measurements in resonance fluorescence," Phys. Rev. A **18**, 201–207 (1978).
20. M. Dagenais and L. Mandel, "Investigation of two-time correlations in photon emissions from a single atom," Phys. Rev. A **18**, 2217–2228 (1978).
21. J. D. Cresser, J. Haeger, G. Leuchs, M. Rateike, and H. Walther, "Resonance fluorescence of atoms in strong monochromatic laser fields," in *Dissipative Systems in Quantum Optics*, Vol. 27 of Topics in Current Physics, R. Bonifacio, ed. (Springer-Verlag, Berlin, 1982), pp. 21–59.
22. R. Short and L. Mandel, "Observation of sub-Poissonian photon statistics," Phys. Rev. Lett. **51**, 384–387 (1983).
23. L. Mandel, "Photon interference and correlation effects produced by independent quantum sources," Phys. Rev. A **28**, 929–943 (1983).
24. A. Aspect, P. Grangier, and G. Roger, "Experimental realization of Einstein–Podolsky–Rosen–Bohm gedankenexperiment: a new violation of Bell's inequalities," Phys. Rev. Lett. **49**, 91–94 (1982).
25. A configuration for generating such light, based on two-photon cascaded emissions, is presented in B.E.A. Saleh and M. C. Teich, "Sub-Poisson light generation by selective deletion from cascaded emissions," Opt. Commun. (to be published).
26. It is interesting to note that the violation of Bell's inequalities was recently shown by Reid and Walls to be associated with nonclassical light (i.e., the nonexistence of a well-behaved positive Glauber P function). See M. D. Reid and D. F. Walls, "Violation of Bell's inequalities in quantum optics," Phys. Rev. Lett. **53**, 955–957 (1984).
27. M. C. Teich, P. R. Prucnal, G. Vannucci, M. E. Breton, and W. J. McGill, "Multiplication noise in the human visual system at threshold: 3. The role of non-Poisson quantum fluctuations," Biol. Cybern. **44**, 157–165 (1982).
28. M. C. Teich, B. E. A. Saleh, and T. Larchuk, "Observation of sub-Poisson Franck–Hertz light at 253.7 nm," in *Digest of the Thirteenth International Quantum Electronics Conference* (Optical Society of America, Washington, D.C., 1984), post-deadline paper PD-A6.
29. D. R. Cox, *Renewal Theory* (Methuen, London, 1962).
30. P. R. Prucnal and M. C. Teich, "Refractory effects in neural counting processes with exponentially decaying rates," IEEE Trans. Syst. Man Cybern. **SMC-13**, 1028–1033 (1983).
31. J. N. Dodd, W. J. Sandle, and O. M. Williams, "A study of the transients in resonance fluorescence following a step or a pulse of magnetic field," J. Phys. B **3**, 256–270 (1970).
32. M. Stock, R. E. Drullinger, and M. M. Hessel, "Comparison between electron beam and optically produced mercury excimer fluorescence," Chem. Phys. Lett. **45**, 592–594 (1977).
33. W. Buhr, W. Klein, and S. Pressler, "Electron impact excitation and UV emission in the Franck–Hertz experiment," Am. J. Phys. **51**, 810–814 (1983).
34. M. C. Teich, J. M. Schroeer, and G. J. Wolga, "Double-quantum photoelectric emission from sodium metal," Phys. Rev. Lett. **13**, 611–614 (1964).